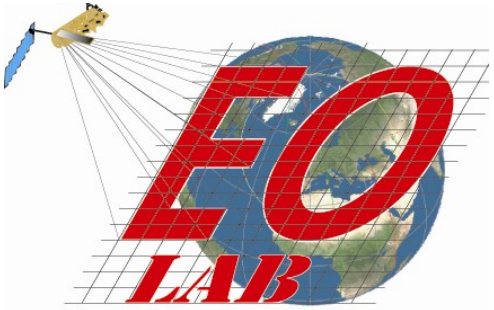

Earth Observation Laboratory

PhD Program in GeoInformation

DISP - Tor Vergata University

Hyperspectral and multi-angle CHRIS Proba images for the generation of land cover maps

Candidate: Riccardo Duca

Mentor: Fabio Del Frate

Final dissertation – 22nd May 2008

Outline

- Introduction

State of the art, thesis objectives.
The CHRIS Proba mission, the test-site, the dataset.

- Image pre-processing

Radiometric correction (drop-out correction and destriping).
Atmospheric correction.

- Multi-angular analysis

- NNs Classification

Classification of hyperspectral CHRIS nadir imagery.
Classification of hyperspectral multi-angular CHRIS imagery.
Further capabilities given by multi-temporal acquisitions.
Comparison with ETM+ acquisitions.

Hyperspectral and multi-directional measurements: the state of art

• Hyperspectral measuremetns have often demonstrated effectiveness for fine classification and Geo/Biophysical variable estimation [*Pearlman et al, 2001*].

• The hyperspectral technology is widely developed for aircraft system (AVIRIS, MIVIS, AHS,…) but still not for satellite platforms (only NASA EO-1 Hyperion operational at the moment).

• Existing satellite missions such as Terra MISR and ADEOS-POLDER are providing systematic spectral and multi-angular data at coarse spatial resolution, especially for aerosols properties retrieval and land applications at very small scale.

• Hyperspectral and multi-directional measurements at high resolution have been produced in airborne campaign (DAISEX and AMTIS) for a limited number of sites and temporal acquisitions [*Berger et al, 2001*], [*Huang et al, 2006*] .

The Proba-1 mission and the small hyperspectral CHRIS

The main objectives regard the developing and the validation of new solution in spacecraft and sensor design.

CHRIS is a small hyperspectral sensor and it is used to measure directional spectral reflectance of land areas, thus allowing new biophysical and biochemical products and information on land surfaces.

- Multiple imaging of same target area under different viewing and illumination geometries
- Spectral range: 415-1050 nm
- Up to 64 bands at 34 m of spatial resolution, selectable spectral sub-configuration at 18 m of spatial resolution
- Frame of 13kmx13km

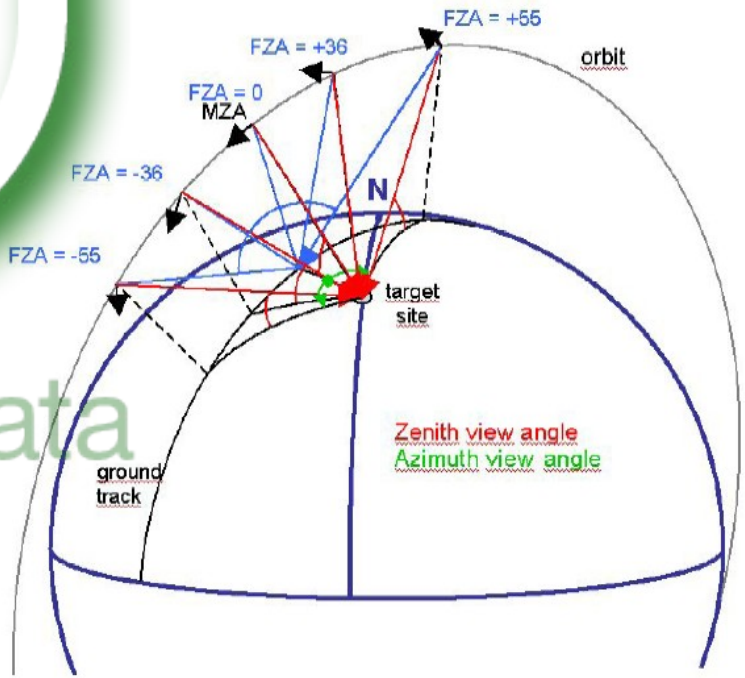

Thesis objectives

• Development of methodologies for the complete treatment of the CHRIS images, from the noise reduction till the top of canopy (TOC) reflectance computation.

• Use of neural network methodology for the production of land cover maps at high spatial resolution starting from CHRIS mode 3 imagery.

• Evaluation of the performance provided by different configurations of the input vector exploiting hyperspectral, multi-angle and multi-temporal measurements.

CHRIS Proba is the first mission which provides over the same sites systematic hyperspectral, multi-angle and multi-temporal measurements.

The test-site of Frascati and Tor Vergata

- Heterogeneous scenario, different surfaces (artificial, natural, different crop types)
- Several data available (remotely sensed, GIS layers, ground truth, ground measurements)

CHRIS images over Frascati and Tor Vergata

Sub set image of 9 October 2006

CHRIS mode 3 (18 bands, 18 m of resolution)

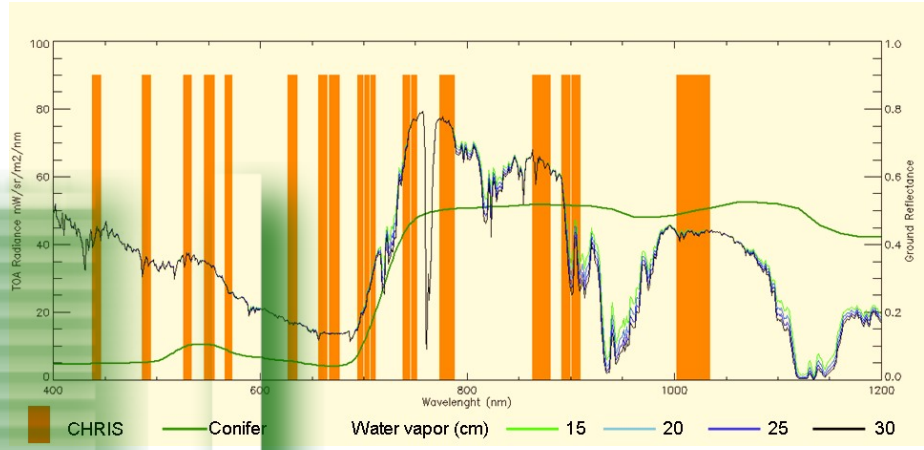

ETM+ 6 bands, 32 m of resolution

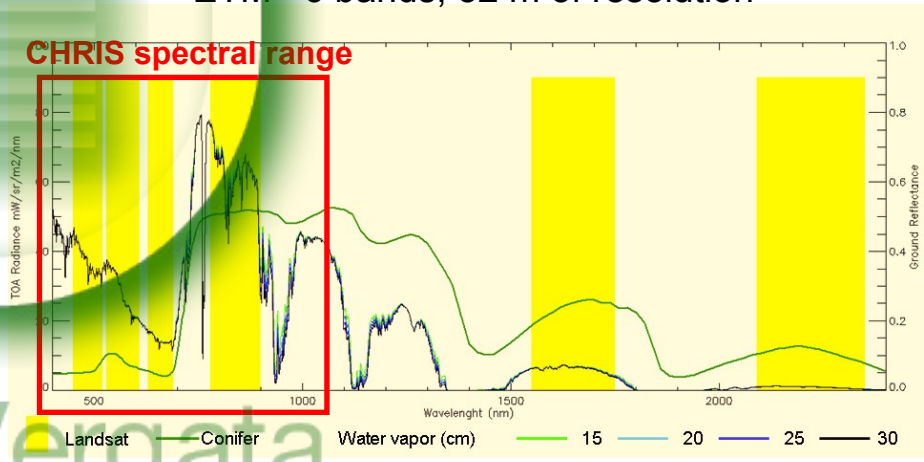

Images:
-10 CHRIS acquisitions mode 3
- 3 ETM Landsat (2001 and 2004)
- 2 VHR Quickbird (2002 and 2005)

Auxiliary data:
- GIS layer of Frascati vineyards
- CLC Lazio
- Aerosols measurements provided by Aeronet project
- Others auxiliary data

CHRIS Images provided by esa cat-1 3075
Others images provided by Baccus/Di Vino projects
CLC and aerosol meas. free available

The removal of radiometric artifacts: black pixels and stripes

Black pixel correction

Pixels with 0 value occur along the rows following a periodic disposition. A filter of 3x3 pixels substitutes the missing values with the average.

Destriping

The stripes noise is due to a residual miscalibration of the detectors. Moreover, the thermal fluctuations produce a not predictable effect making difficult an absolute satisfactory calibration.

- The noise appears in the images as along-track stripes.
- The correction factors have to be estimated for each acquisition.
- The correction becomes strongly “image dependent”.

Principal methodologies:

- Statistical spatial filtering, advanced filtering
- Histogram matching
- Histogram modification through the statistical calculation of the correction factors (DIELMO – UV method) [*Garcia and Moreno, 2004*]

Destriping by the low-pass filtering in the spatial frequency domain: the methodology

The main steps have been traced by M.J.Settle [Settle, 2004]

3. For each band, calculate an average radiance for each column, calculate the logarithm.
4. Apply a low pass filter to cut the high frequency components.
5. Subtract the result of step 3 from the logarithm of averages to obtain the correction factors for each column.
6. Calcolate the anti-logarithm and apply the correction factors.

MY MAIN IMPROVEMENTS

- The filtering is applied in the frequency spatial domain (FFT over the column averages).
- The filter is a Butterworth low-pass. The parameters are tunable to improve the correction.
- Not all the pixels are considered in the averages. Dark and bright pixels are masked, improving the correction over not homogeneous areas.
- The new range for the average calculation is defined in function of the column standard deviation.

Destriping by the low-pass filtering in the spatial frequency domain: the results

• The visual assessment confirms a good correction for all the images considered for this studies. The image statistics are satisfactory preserved.

• The masking technique of dark and bright areas is providing reasonable improvements for the correction.

• The correction is satisfactory with the respect to others implemented methodologies [*Cutter, November 2006*]

• Residual uncorrected stripes, visible as blurred along track shadows, are still present in scenarios characterized by the presence of heterogeneous surfaces (for example land/sea).

Not corrected

Corrected

Bright spot masked

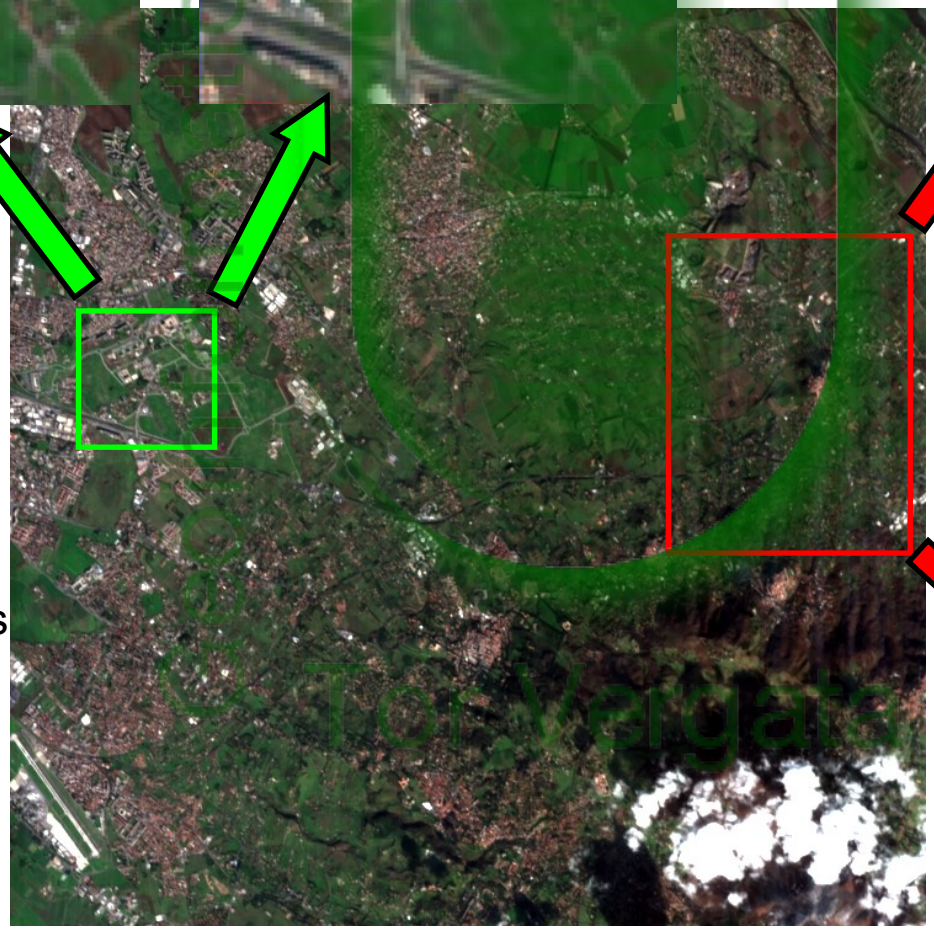

Bright spot not masked

<u>Frascati and Tor Vergata</u>

Satisfactory correction for this scenario, also in presence of clouds and shadows

Acquisition of January 2007

Lybian desert
Evident correction for the band1, mostly corrupted by the noise

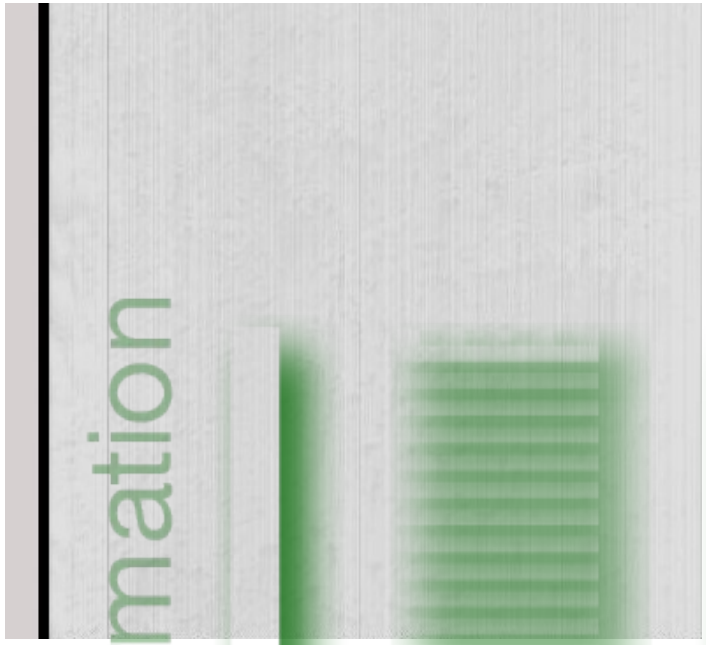

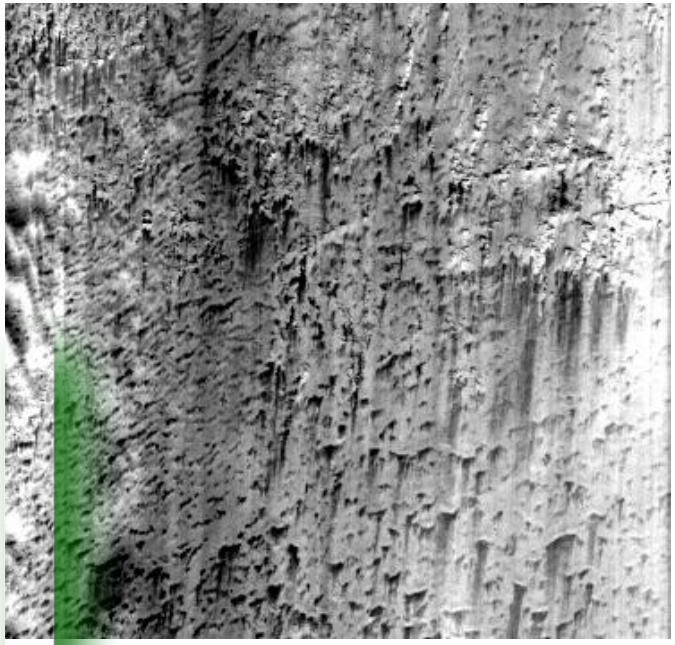

Tampa Bay (USA)
Residual noise for columns characterized by sea/land mixed pixels

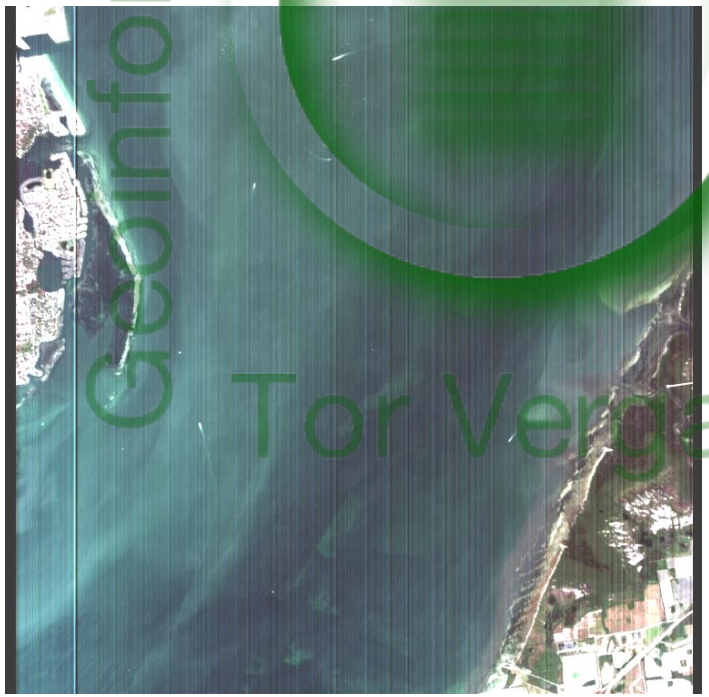

Atmospheric correction and reflectance computation (I)

It aims at minimizing the effects of the atmospheric and aerosols contribution in the measured radiance.

- Crucial for the retrieval of spectral signatures by the use of hyperspectral measurements.
- Essential for multi-directional and multi-temporal analysis.
- The correction needs a complete characterization of the radiative quantities which are related to the atmospheric properties of the site.

METHODOLOGY

1 The atmospheric radiance, the direct and diffuse transmittance and the total irradiance are simulated by the use of LibRadtran suite for the radiative transfer simulation [*Mayer et al, 2005].*

The aerosols measures available under the AERONET project have been considered for this area (measurements performed by CNR Tor Vergata).

Atmospheric correction and reflectance computation (II)

2 The simulated LUTs are compared with the radiances extracted for some surfaces of reference (principally asphalted surfaces)

3 The correction is performed using the relation which links the TOC reflectance with the TOA radiance

$$\rho(\lambda,\theta) = \frac{\pi(L_{TOA}(\lambda,\theta) - L_{path}(\lambda,\theta))}{E_0(\lambda,\zeta)\,T(\lambda,\theta)}$$

4 The adjacency effects are compensated using a weighted mean [*Vermonte et al, 1996*]

$$\rho^2(x,y) = \rho^1(x,y) + q\{\rho^1(x,y) - \overline{\rho}(x,y)\} \qquad \overline{\rho}(x,y) = \frac{1}{N^2}\sum_{i,j}^{N} \rho^1_{i,j}(x,y)$$

Final results

Asphalted surface

Radiance top of the atmosphere

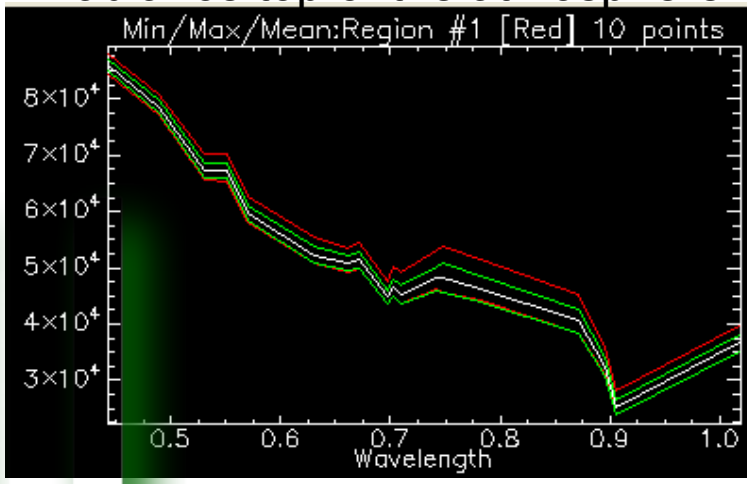

Reflectance after the correction

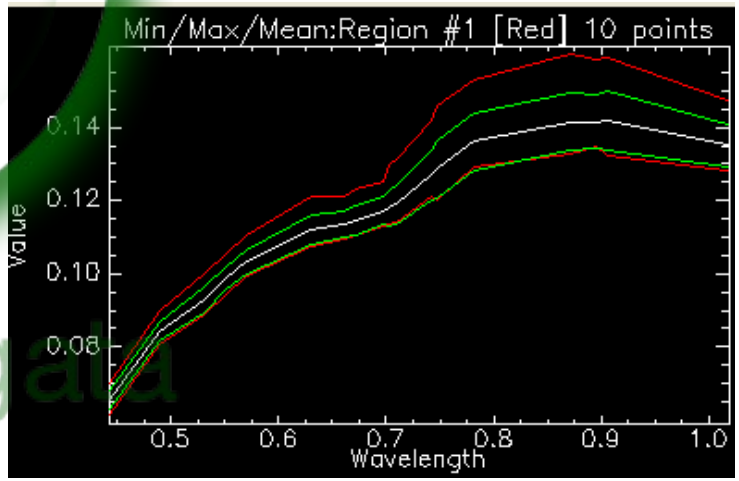

Mitigation of adjacency effects

Multi-angle acquisitions: visual assessment

- Multi-angle band 10 composition (703 nm)

RGB

FZA: -36, 0, 36

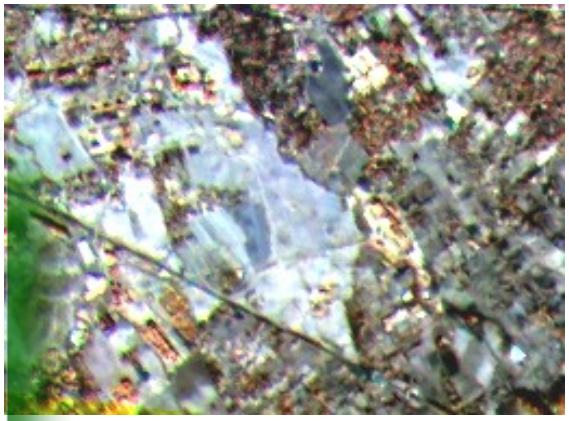

FZA: 0, 36, 55

- Anisotropies are observed in general for soil, vegetation and different artificial structures

Single-angle RGB

Multiangle RGB

VHR image

<u>The case of cultivated fields</u>

The multi-angle composition can better highlight spectral differences in the cultivated fields

Multi-angle acquisitions: reflectance analysis

Crops and natural areas

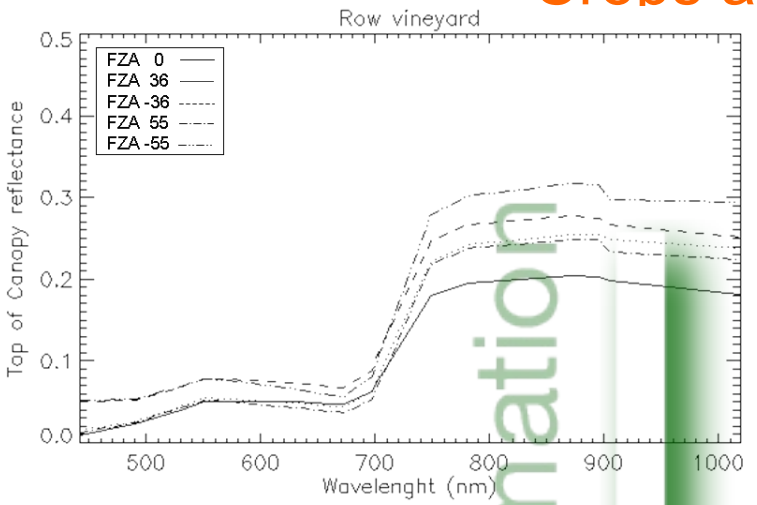

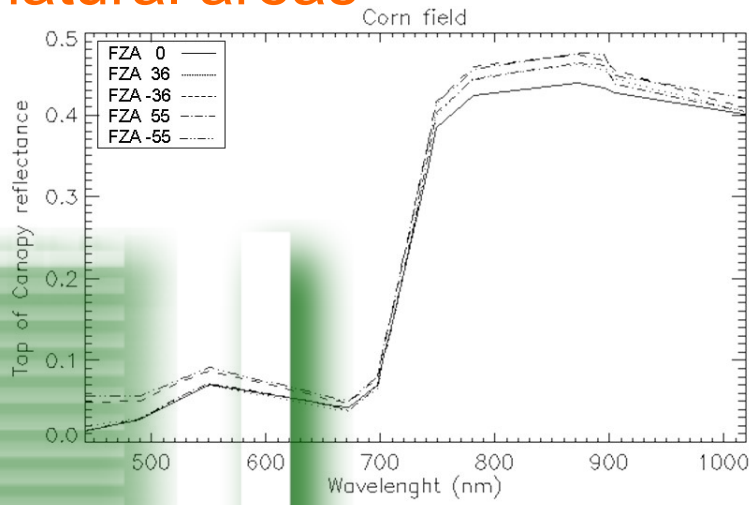

- Differences on the angular reflectance have been observed for crops with a particular structure of plants and canopies

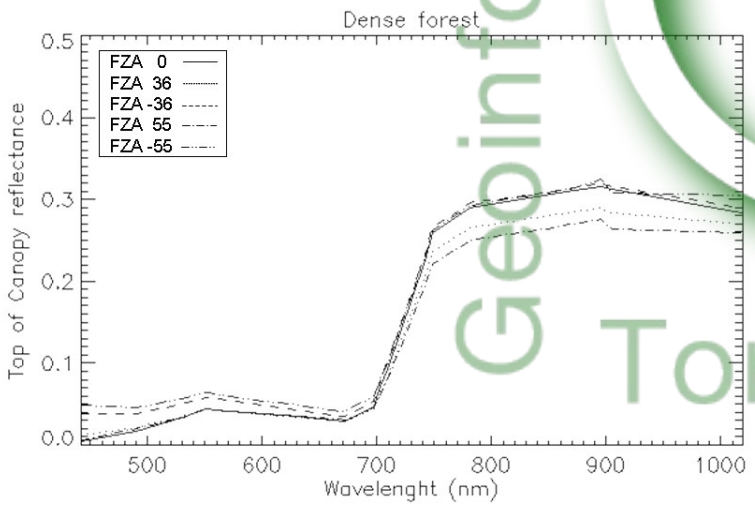

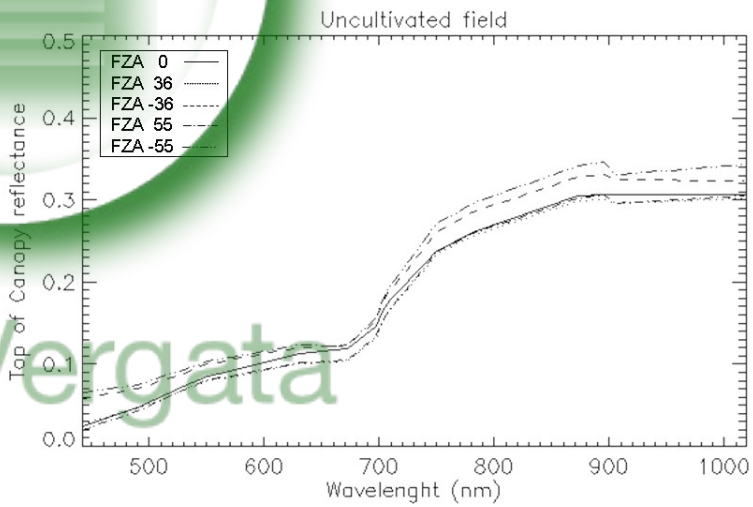

- Vegetation and areas without a significant geometric characterization have a low sensitivity to the angle of view

Multi-angle acquisitions: reflectance analysis

Man made surfaces

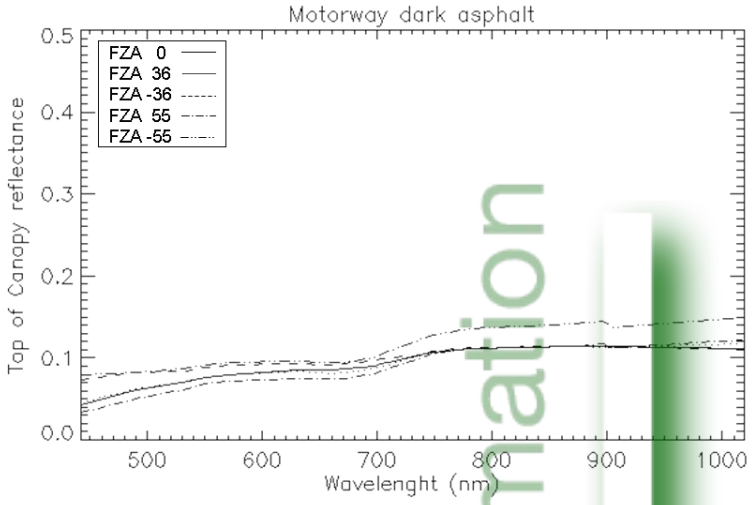

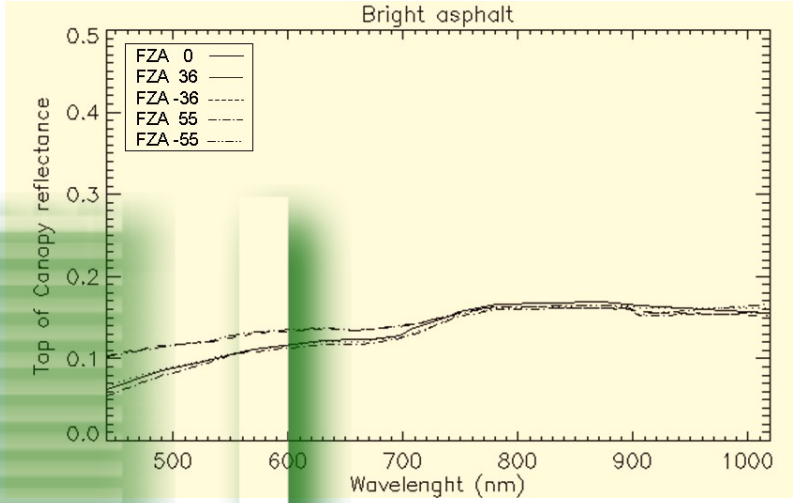

- Asphalted and flat surfaces have the lowest sensitivity to the angle of view

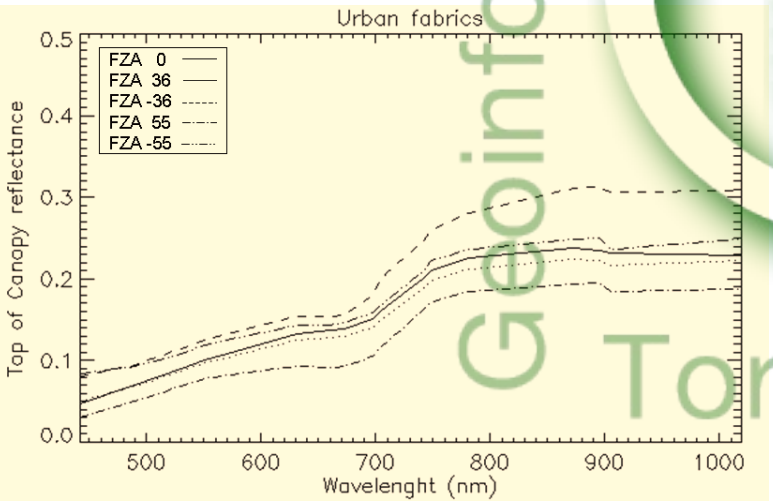

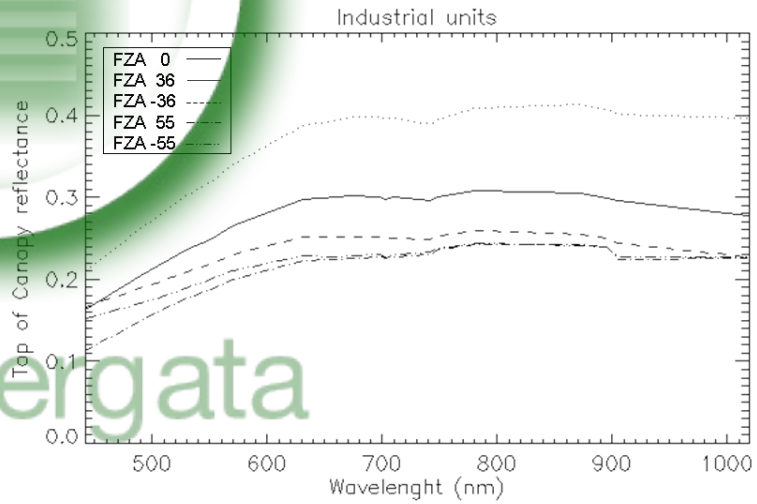

- Urban buildings and big structures have a very important dependence with respect to direction of acquisition

The pixel based neural network classification for the CHRIS Proba imagery

- The neural network classification scheme is based on the multi-layers perceptron (MLP) configuration.

- Learning process carried out considering two dataset: training and test set.

- Best configurations found when the error function reaches its minimum value on the test set.

- The minimization of the error function is pursued considering the Scaled Coniugate Gradient (SCG)

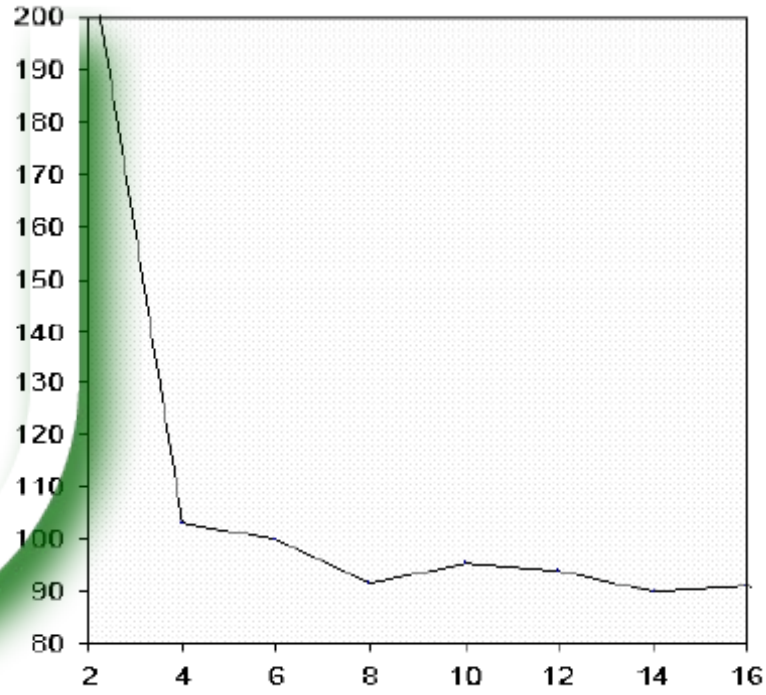

The pixel based neural network classification for the CHRIS Proba imagery

1. Classification of the hyperspectral nadir image.
2. Classification performed by the use of multi-directional images.
3. Classification of joined multi-temporal and multi-directional images

Classification of the nadir image

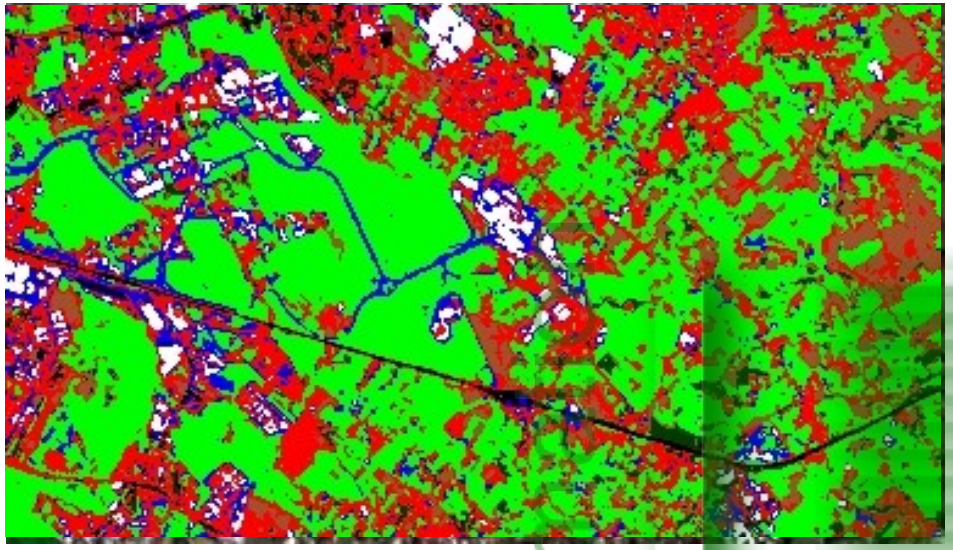

Dark gray asphalt
Bright gray asphalt
Urban fabric roofs
Commercial-Industrial units
Bare soil
Green vegetated areas
Forest

Seven classes of land cover have been individuated for this scenario according to their spectral properties ad to the seasonal characterization of vegetated areas and crops

	GROUND TRUTH						
	Dark Asphalt	Bright Asphalt	Urban Buildings	Industrial and commercial units	Bare soil	Green vegetated areas	Forest and permanent crops
Dark Asphalt	85.4	4.6	1.0	0.0	0.2	0.0	0.0
Bright Asphalt	0.3	53.8	6.4	1.5	0.0	0.1	0.0
Urban Buildings	10.1	27.0	84.0	1.5	29.5	0.0	0.0
Industrial/commercial units	0.0	14.3	0.7	97.0	0.0	0.0	0.0
Bare soil	2.1	0.3	6.1	0.0	70.1	1.9	7.3
Green vegetated areas	0.0	0.0	1.8	0.0	0.1	98.0	9.1
Forest and permanent crops	2.1	0.0	0.0	0.0	0.1	0.0	83.6

Net topology 18/14/14/7

Overall Accuracy = 85%
Kappa Coefficient = 0.82

More than 6000 pixels used as validation points

Classification of the nadir image

Dark gray asphalt
Bright gray asphalt
Urban fabric roofs
Commercial-Industrial units
Bare soil
Green vegetated areas
Forest

Seven classes of land cover have been individuated for this scenario according to their spectral properties ad to the seasonal characterization of vegetated areas and crops

	GROUND TRUTH						
	Dark Asphalt	Bright Asphalt	Urban Buildings	Industrial and commercial units	Bare soil	Green vegetated areas	Forest and permanent crops
Dark Asphalt	85.4	4.6	1.0	0.0	0.2	0.0	0.0
Bright Asphalt	0.3	53.8	6.4	1.5	0.0	0.1	0.0
Urban Buildings	10.1	27.0	84.0	1.5	29.5	0.0	0.0
Industrial/commercial units	0.0	14.3	0.7	97.0	0.0	0.0	0.0
Bare soil	2.1	0.3	6.1	0.0	70.1	1.9	7.3
Green vegetated areas	0.0	0.0	1.8	0.0	0.1	98.0	9.1
Forest and permanent crops	2.1	0.0	0.0	0.0	0.1	0.0	83.6

Net topology 18/14/14/7

Overall Accuracy = 85%
Kappa Coefficient = 0.82

More than 6000 pixels used as validation points

Multi-angle classification

- The same acquisition of 28 th February 2006 has been considered. FZA0, FZA-36 and FZA+36 have been integrated as additional multi-angular information.

- A new NN has been trained with the same training and test set of the nadir classification.

- Results validated with the same collection of points of the previous classification.

Net Topology 54/24/24/7

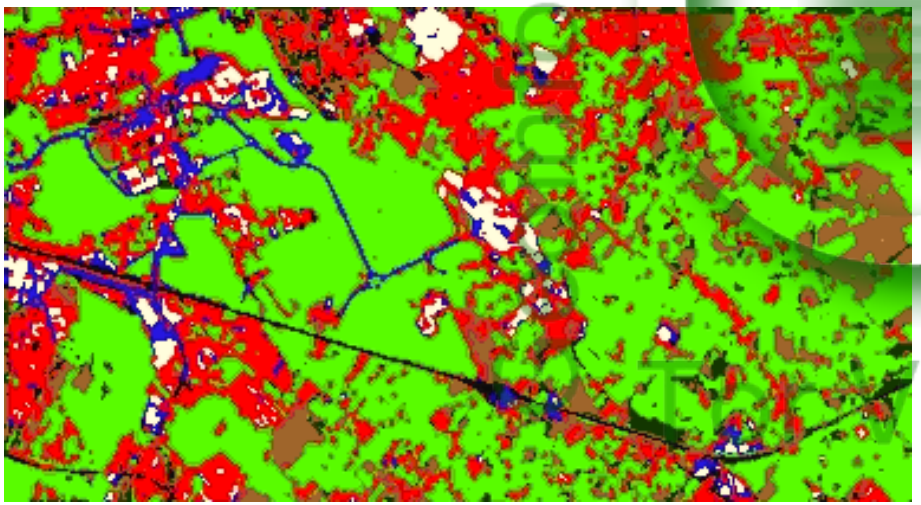

Dark gray asphalt
Bright gray asphalt
Urban fabric roofs
Commercial-Industrial units
Bare soil
Green vegetated areas
Forest

Accuracy of 92%, Kappa Coefficient = 0.91
+7% respect to the nadir image using the same pixels of ground truth

Visual and statistical assessment

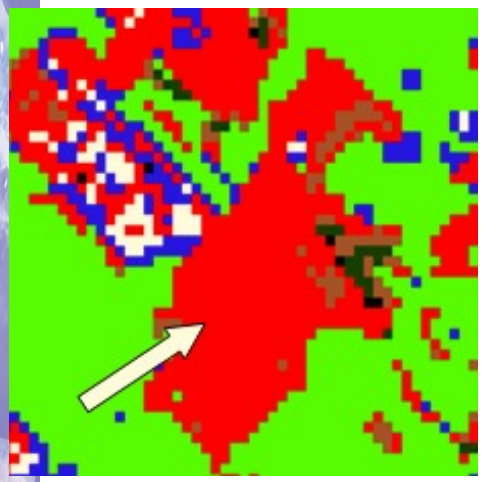

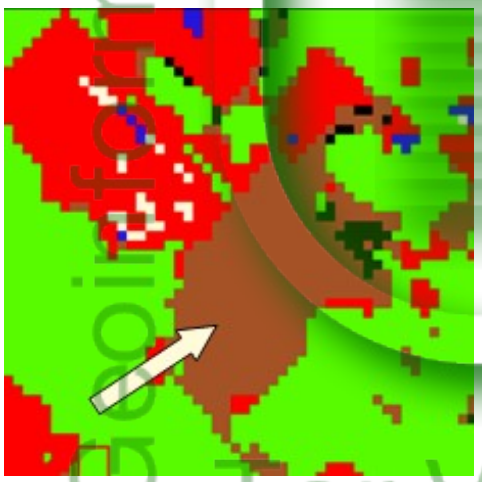

Single view

Multi-angle

Example of a solved ambiguity

Bare soil/urban buildings

SURFACE	IMPROVEMENTS
Dark Asphalt	-3%
Bright Asphalt	+27%
Urban buildings	+10%
Industrial/commercial units	Not relevant
Bare soil	+19%
Green vegetated areas	Not relevant
Forest and permanent crops	Not relevant

Potential sources of errors:

- Not satisfactory local co-registration for some areas
- Distortions due to a very large angles of acquisition

- Small features could be confused
- Structures not well segmented
- Sparse small structures deleted

Single angle VS multi-angle: Comments

- The multi-directional information has provided a reasonable improvement in the classification process around the 7%.

- Improvements are observed especially for urban structures, in particular for asphalted surfaces and urban buildings.

- Bare soils are better classified and the ambiguity with some classes is strongly mitigated.

- Not relevant improvements have been observed in vegetated areas without a particular geometric structure such as very dense forest, grasslands and some types of crop.

- Acquisitions like FZA -55 and +55 can not be considered because geometrically distorted and dominated by strong atmospheric affects.

- The integration of multi-angle acquisitions often requires a difficult co-registration and a degradation of the spatial resolution.

Further potential given by multi-temporal acquisitions: preliminary analysis

• Systematic and multi-temporal hyperspectral measurements permit the monitoring of the spectral evolution of some surfaces.

• The analysis has confirmed that the reflectance of vegetated surfaces changes during the year in function of the crop/vegetation type, status of the cultivation and man actions.

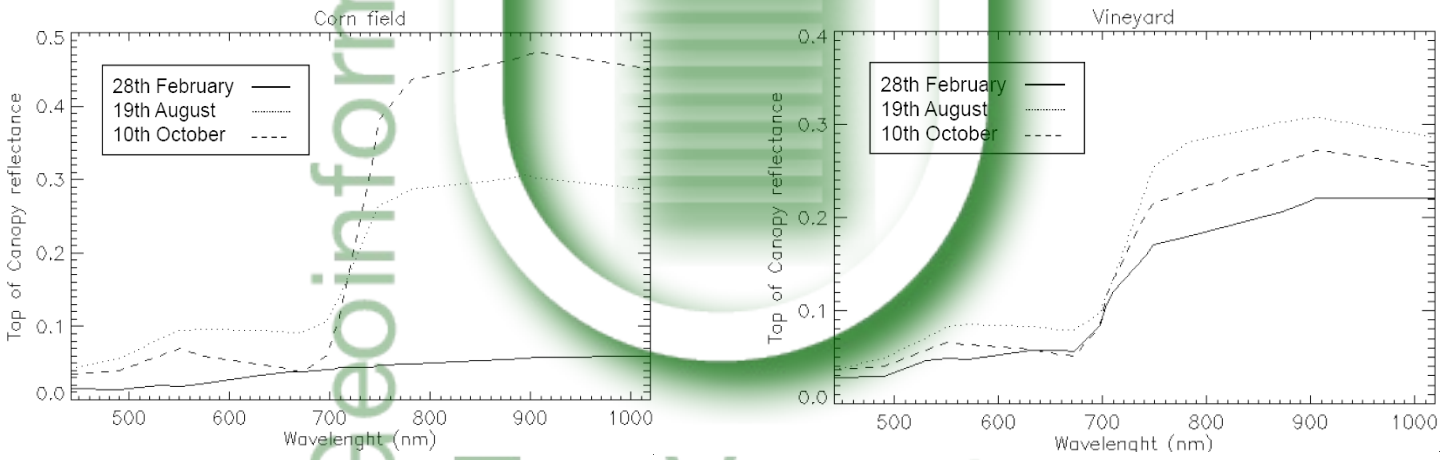

• These spectral changes, as well as the multi-directional information, can be provided to the classification process in order to discriminate crops and others types of vegetated surfaces.

Further potential given by multi-temporal acquisitions: the methodology

• Three dates have been selected according to some requirements: seasonal sampling, frames extent, cloud cover, difficult registration, angle of view.
• The exercise considers an hyperspectral and multi-temporal classification and also an hyperspectral multi-temporal/angular one.

Multitemporal
28 February FZA0
19 August FZA0
09 October FZA0

Multi-temporal and multi-angle
28 February FZA0
19 August FZA0
19 August FZA36
09 October FZA0

• Geometric and cloud cover constraints have limited the angular information to the FZA 36 acquisition of the summer image.

• The NN training has been performed using the same patterns for both the exercises.

Further potential given by multi-temporal acquisitions: the methodology

• Three dates have been selected according to some requirements: seasonal sampling, frames extent, cloud cover, difficult registration, angle of view.
• The exercise considers an hyperspectral and multi-temporal classification and also an hyperspectral multi-temporal/angular one.

Multitemporal
28 February FZA0
19 August FZA0
09 October FZA0

Multi-temporal and multi-angle
28 February FZA0
19 August FZA0
19 August FZA36
09 October FZA0

• Geometric and cloud cover constraints have limited the angular information to the FZA 36 acquisition of the summer image.

• The NN training has been performed using the same patterns for both the exercises.

Further potential given by multi-temporal acquisitions: the methodology

- Three dates have been selected according to some requirements: seasonal sampling, frames extent, cloud cover, difficult registration, angle of view.
- The exercise considers an hyperspectral and multi-temporal classification and also an hyperspectral multi-temporal/angular one.

Multitemporal
28 February FZA0
19 August FZA0
09 October FZA0

Multi-temporal and multi-angle
28 February FZA0
19 August FZA0
19 August FZA36
09 October FZA0

- Geometric and cloud cover constraints have limited the angular information to the FZA 36 acquisition of the summer image.

- The NN training has been performed using the same patterns for both the exercises.

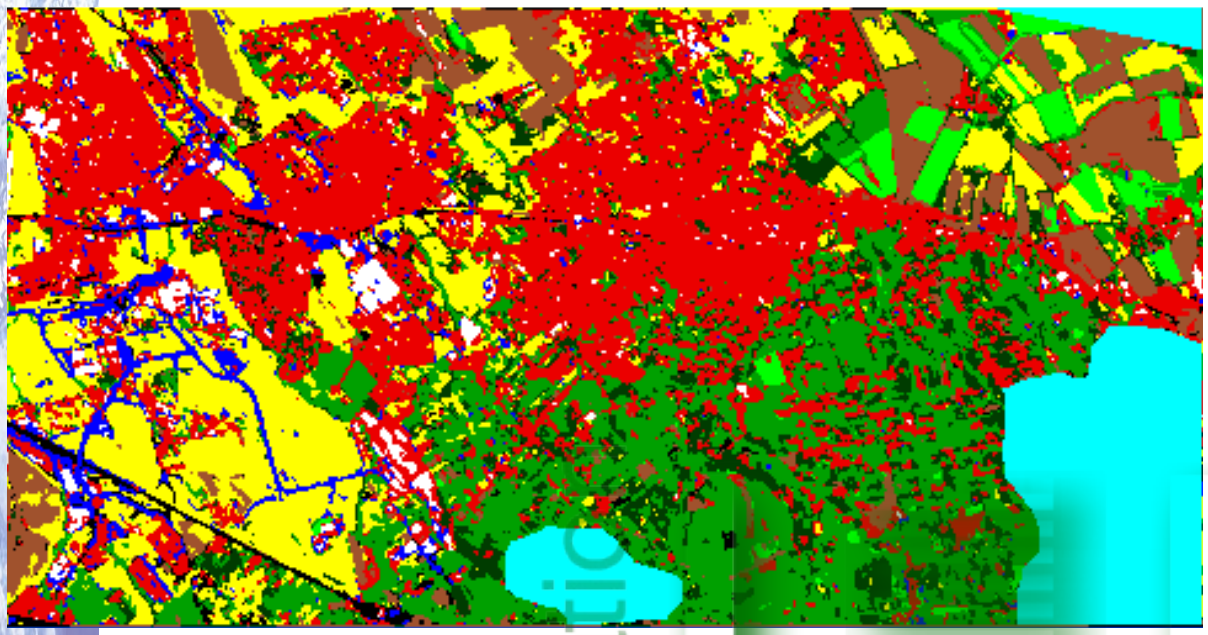

Dark Asphalt
Bright Asphalt
Urban Fabrics
Industrial Units (white)
Uncoltivated
Permanent Crops Trees
Permanent Crops Vineyards
Corn Fields
Agricultural
Clouds and Shadows

Ground truth of 21700 pixels

- Multi temporal: 54/20/20/14, accuracy of 87.7% Kappa Coefficient = 0.84
- Multi-temporal +angle: 72/18/18/14, accuracy of 92.9% Kappa Coefficient = 0.91

	GROUND-TRUTH								
	Dark Asphalt	Bright asphalt	Urban Buildings	Industrial/ Commercial Units	Uncultivated	Other permanent crops	Vineyards	Corn	Other agricultural areas
Dark Asphalt	88.73	1.41	0.04	0.44	0.04	0	0.06	0	0
Bright Asphalt	1.41	92.94	0.92	0.66	0.23	0	0.02	0	0
Urban Buildings	4.93	4	96.21	4.18	0.27	0	2.31	0.16	4.78
Industrial/ Commercial Units	0	1.41	2.2	94.73	0	0	0	2.02	0
Uncultivated	4.93	0.24	0.35	0	86.41	1.71	5.1	0.08	0
Other permanent crops	0	0	0.13	0	3.32	82.91	15.7	0.00	0
Vineyards	0	0	0.15	0	5.67	14.1	73.02	2.58	0.55
Corn	0	0	0	0	3.57	0.21	3.54	95.16	0.1
Other agricultural areas	0	0	0	0	0.49	1.07	0.26	0.00	94.56

SURFACE	IMPROVEMENTS
Dark Asphalt	+6%
Bright Asphalt	-2%
Urban Buildings	Not relevant
Industrial/commercial units	Not relevant
Uncultivated	+8%
Other permanent crops	+1%
Vineyards	+11%
Corn	+2%
Other agricultural areas	+4%

Multi-temporal vs Multi-temporal,Multi-angular: comments

• Hyperspectral and multi-temporal acquisitions have permitted to identify crops, cultivated areas and others vegetated surfaces inside the macro class “vegetation”.

• Also surfaces characterized by a stable spectral signature (the urban classes) have received an improvement in the classification accuracy.

• Also in this case the multi-directional information has provided significant improvements, especially for the crops discrimination.

• The co-registration, the atmospheric correction and the signature calibration remain crucial steps for the processing.

Landsat ETM+ vs. Proba CHRIS

A comparison in terms of land cover accuracy has been done considering two acquisitions related to the same season.

ETM+ 19 August 2004

CHRIS 19 August 2006

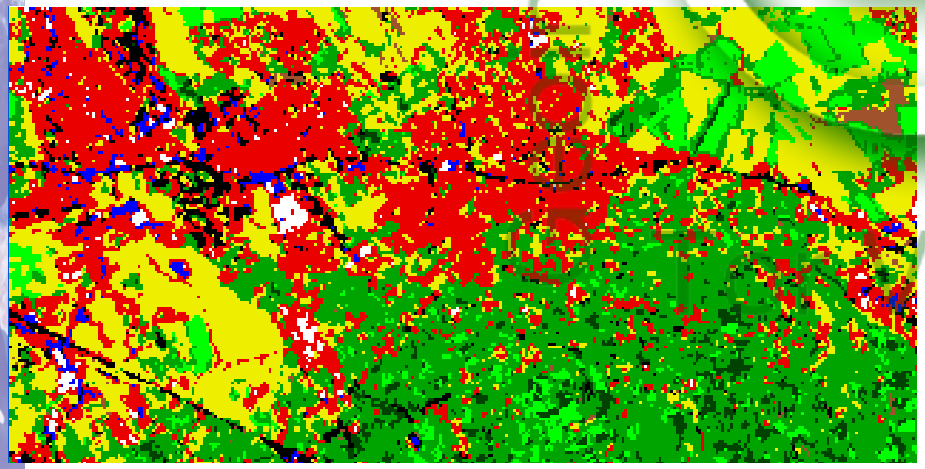

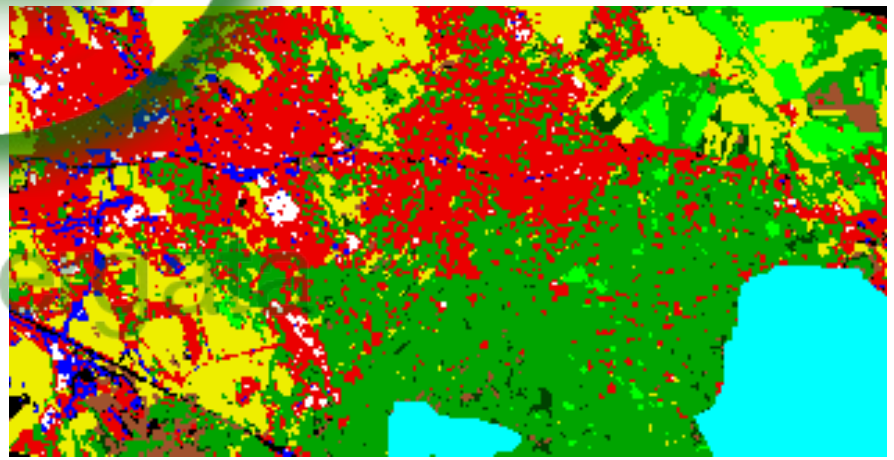

Classification comparison: the results

- CHRIS can better differentiate surfaces and classes inside the macro class “urban”.
- ETM can well identify agricultural areas, but for crops discrimination the hyperspectral measurements can provide better results.
- Uncertainties remain for the identification among uncultivated, vineyard and some urban buildings due to the similarity of the spectral reflectance. In several cases ETM has provided better results.

CHRIS overall accuracy 79.8%
Kappa Coefficient = 0.73

ETM+ overall accuracy 73.2%
Kappa Coefficient = 0.66

Uncultivated Vineyard Urban buildings

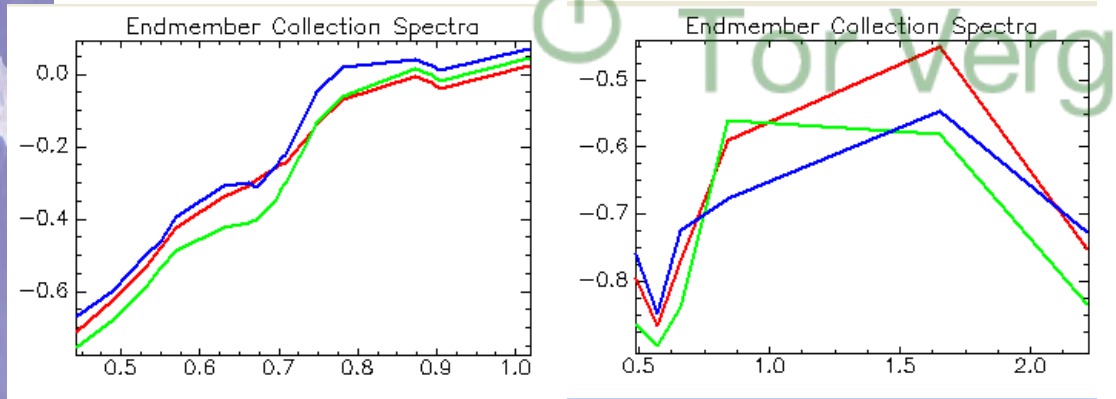

Improvements of CHRIS with respect to ETM

Dark Asphalt	+15
	+25
Bright Asphalt	Similar
Urban Fabrics	+20
Industrial Units (white)	Similar
Permanent Crops Trees	+15
Vineyards	+5
Corn Fields	
Uncultivated	Similar
Bare Soil	+16

Study conclusions (I)

A complete treatment of hyperspectral, multi-angular, multi-temporal CHRIS imagery for “end-to-end” applications has been carried out.

The design of optimum classifying schemes required several steps:

- Elimination of radiometric artifacts
- Removal of atmospheric effects using a radiative transfer model
- Co-registration of up to 72 multi-angular, multi-temporal images
- Design of suitable neural network topologies

The simultaneous use of multi-angle and hyperspectral measurements allowed us an overall accuracy of about 92% considering 7 land cover classes, with an improvement of almost 7% with respect to the single nadir acquisition.

The additional exploitation of the information brought in by multi-temporal data led to overall accuracies of about 93% considering 9 different classes

Study conclusions (II)

The study demonstrates once again the effectiveness of neural network algorithms in positively combining different levels of information

When more multi-temporal acquisitions will be available during one year and over the same test site, a procedure for the selection of the inputs to the network will be unavoidable to eliminate unnecessary or misleading quantities

R.Duca, F.Del Frate, *:"Hyperspectral and multi-angle Chris Proba Images for the generation of land cover maps"*, accepted for publication on IEEE TGRS

The evolution of multi-spectral sensors: Sentinel-2

Activities developed at ESTEC (8 months):

•Contribution to the developing of SEN2 simulator

• Generation of simulated images over several scenarios using hyperspectral airborne images

• Contribution to the assessment of the new potentialities of Sentinel-2

• Evaluation of the spatial and radiometric artifacts due to the on-board compression (wavelength based)

• Contribution to the assessment concerning the baseline parameters of the processing

• Land cover maps

Results presented at:

IGARSS 07 (F.Gascon)

ESA Bulletin special GMES (P.Martimort et al.)

Others workshop (P.Martimort et al.)

This work is continuing: 1 MD thesis (F.Ramoino), IGARSS08

Other publications:

F.Del Frate, R.Duca, D.Solimini: *"Urban features retrieved by hyperspectral multi-angle CHRIS/Proba images"*, URBAN 2007
F.Del Frate, R.Duca, D.Solimini: *"The potential of hyperspectral and multi-angle CHRIS/Proba images in vegetation identification and monitoring"*, Envisat Symposium 2007
F.Del Frate, R.Duca, D.Solimini: *"Use of CHRIS/Proba Images for land use product"* Proceeding IGARSS 2007

Others activities:

- Seminars: TVU Geo-seminar (2006), ESTEC final presentation, ESA Tsunami dataset presentation.
- Lectures at CM2, MS, TDE, several ESRIN courses for ESA educational activities
- Tutorship: bachelor (2) and MD thesis (1).